

# Aldose reductase inhibitors for diabetic complications: Receptor induced atom-based 3D-QSAR analysis, synthesis and biological evaluation



Bhawna Vyas<sup>a</sup>, Manjinder Singh<sup>b</sup>, Maninder Kaur<sup>b</sup>, Malkeet Singh Bahia<sup>b</sup>, Amteshwar Singh Jaggi<sup>c</sup>, Om Silakari<sup>b</sup>, Baldev Singh<sup>a,\*</sup>

<sup>a</sup> Department of Chemistry, Punjabi University, Patiala 147002, Punjab, India

<sup>b</sup> Molecular Modeling Lab (MML), Department of Pharmaceutical Sciences and Drug Research, Punjabi University, Patiala 147002, Punjab, India

<sup>c</sup> Division of Pharmacology, Department of Pharmaceutical Sciences and Drug Research, Punjabi University, Patiala 147002, Punjab, India

## ARTICLE INFO

### Article history:

Accepted 26 March 2015

Available online 3 April 2015

### Keywords:

Atom-based 3D-QSAR

Docking analysis

Aldose reductase (ALR2)

Flavonoid derivatives

Diabetic complications

## ABSTRACT

Herein, atom-based 3D-QSAR analysis was performed using receptor-guided alignment of 46 flavonoid inhibitors of aldose reductase (ALR2) enzyme. 3D-QSAR models were generated in PHASE programme, and the best model corresponding to PLS factor four (QSAR<sub>4</sub>), was selected based on different statistical parameters (*i.e.*,  $R^2_{\text{train}}$ , 0.96;  $Q^2_{\text{test}}$  0.81; SD, 0.26). The contour plots of different structural properties generated from the selected model were utilized for the designing of five new congener molecules. These designed molecules were duly synthesized, and evaluated for their *in vitro* ALR2 inhibitory activity that resulted in the micromolar ( $\text{IC}_{50} < 22 \mu\text{M}$ ) activity of all molecules. Thus, the newly designed molecules having ALR inhibitory potential could be employed for the management of diabetic complications.

© 2015 Elsevier Inc. All rights reserved.

## 1. Introduction

Worldwide, diabetes is achieving higher dimensions due to change in people life style, which lead to reduced physical activity and increased obesity, the main roots of diabetic conditions. As per world health organisation (WHO) diabetes webpage, 347 million people have diabetes, which is projected to be the 7th leading cause of deaths by 2030 [1]. Diabetes mellitus is one of the most common chronic metabolic diseases, characterized by chronic hyperglycaemia and the development of diabetes-specific microvascular and macrovascular pathology. Prolonged hyperglycemia is a primary causal factor of several diabetic complications. Large prospective clinical studies show a strong relationship between glycaemia and diabetic microvascular complications in both type 1 and type 2 diabetes [2,3].

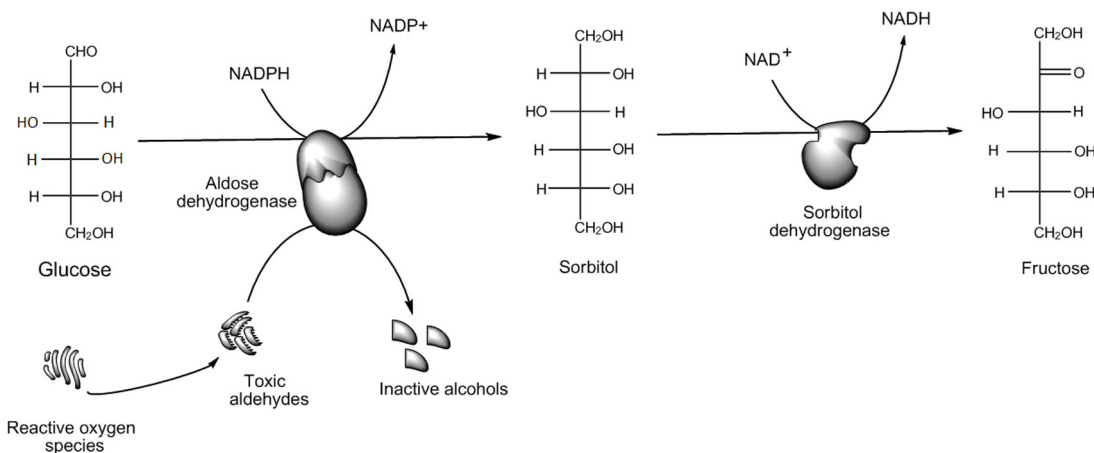
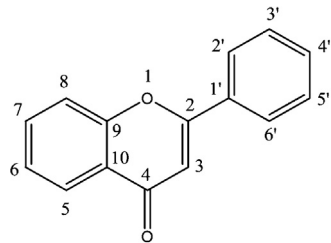
Many studies have revealed a correlation between glucose metabolism via the polyol pathway (Fig. 1) and long-term diabetic complications. Aldose reductase, ALR2 (EC 1.1.1.21), is the first and rate-limiting enzyme in this pathway which normally reduces glucose to sorbitol using Nicotinamide adenine dinucleotide phosphate (NADPH) as a cofactor; at the same time another enzyme

sorbitol dehydrogenase oxidizes sorbitol to fructose. However, in diabetic condition, the glucose level in this pathway is increased and sorbitol is produced faster than being oxidized to fructose [4]. The accumulated sorbitol cannot cross the cell membrane easily and therefore causes swelling and cell dysfunction in a number of tissues. In addition, fructose can become phosphorylated to fructose-3-phosphate, which is broken down to 3-deoxyglucosone, ultimately forming advanced glycation end products that are capable of cellular damage [5–7]. These abnormal metabolic results have been reported to be responsible for diabetic complications such as cataracts [8], retinopathy [9], neuropathy [10], and nephropathy [11]. The inhibition of ALR2 is a possible prevention or treatment of these effects [12].

The flavonoids are of low molecular weight plant products which are abundant, ubiquitously found in a wide variety of edible plants, fruits, nuts, seeds, and plant-derived beverages, such as juice and tea [13]. They are also called vitamin P<sup>16</sup> and have been described as health-promoting, disease-preventing dietary supplements [14]. They are relatively simple to synthesize and extremely safe and associated with low toxicity, making them excellent candidates for several interesting biological activity profiles in enzymatic systems, and as chemo-preventive agents [15]. They may exert an anti-hyperglycaemic effect by promoting peripheral utilization of glucose or enhancing the sensitivity of insulin in diabetic animals [16]. In addition, it was reported that the therapeutic benefits

\* Corresponding author. Tel.: +91 9815988501.

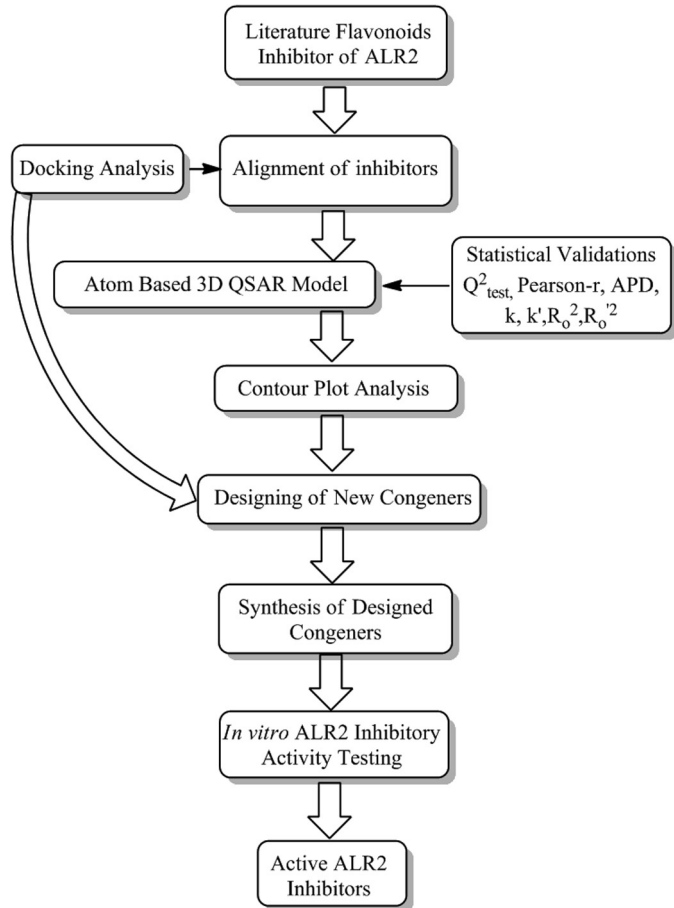
E-mail address: [bhawnaom@rediffmail.com](mailto:bhawnaom@rediffmail.com) (B. Singh).

**Fig. 1.** The polyol pathway.**Fig. 2.** Common template of phenyl-benzopyrane present in data set molecules.

of flavonoids are usually linked to two properties: (i) inhibition of certain enzymes such as xanthine oxidase, ALR2 [17], acetylcholinesterase [18], Janus kinase [19], Spleen Tyrosine Kinase [20] and (ii) antioxidant activity [21], consequently their study is greatly interested in many research fields.

Major pharmaceutical companies pay their attention to the speed up efficacious drug discovery with the primary aim of reducing cost per synthesized compound. Computer aided drug design (CADD) approaches which are able to predict the biological activities of compounds by their structural properties are powerful tools to design new active molecules. In this sense, quantitative structure–activity relationship (QSAR) studies have been successfully applied for modelling biological activities of natural and synthetic chemicals. QSAR studies have been carried out for modelling activities of several kinds of ALR2 inhibitor. Some recent reports have linked structural features of the ligands with their ALR2 inhibition by using topology indexes [17,22] three dimensional (3D)-QSAR methodologies [23,24], comparative molecular field analysis (CoMFA), comparative molecular similarity indices analysis (CoMSIA) and artificial neural networks, etc. [25–27].

The current study involves the development of in silico models to predict the ALR2 inhibitory activity of a set of 46 flavonoids [17] mentioned in Table 1 and the common scaffold of these molecules is displayed in Fig. 2. Stefanic-Petek et al. reported a QSAR model for describing these compounds by using multi-linear regression analysis with classical and quantum chemical descriptors [28]. After that, Fernandez et al. reported linear and nonlinear QSAR models [29], and found that structural features related to the molecular topologies and charges are related to the inhibitory activity of these compounds. Caballero in 2010 reported 3D-QSAR by CoMFA and CoMSIA and Pharmacophore by GALAHAD (genetic algorithm with linear assignment of hyper-molecular alignment of the database) [30]. In the present paper, ALR2 structure guided atom based 3D-QSAR model was developed for throwing some light on the substituent requirements for lead optimization of flavones based

**Fig. 3.** Schematic view of the research protocol followed in the present study.

ALR2 inhibitor. A schematic workflow of proposed study is shown in Fig. 3.

## 2. Experimental

### 2.1. Selection and preparation of molecular dataset

A data set of 46 studied flavone inhibitors of ALR2 was selected from the published literature [17]. The ALR2 inhibitory activity of the selected molecules was reported as  $\text{IC}_{50}$  value in the literature, which corresponds to the negative logarithm of dose

**Table 1**

Molecular structures and their corresponding experimental biological activity values of flavonoid ALR2 inhibitors.

Sr. No.	3	5	6	7	8	2'	3'	4'	5'	pIC <sub>50</sub> <sup>a</sup>
1	OCH <sub>3</sub>	OH	OCH <sub>3</sub>	OH			OH	OH		7.55
2		OH	OCH <sub>3</sub>	OH	CH <sub>2</sub> Ph		OH	OH		7.47
3		OH	OCH <sub>3</sub>	OCH <sub>3</sub>			OH	OH		7.41
4		OCH <sub>3</sub>		OCH <sub>3</sub>	OCH <sub>3</sub>		OH	OH		7.35
5	OCH <sub>3</sub>	OH	OH	OH			OH	OH		7.24
6		OH	OH	OCH <sub>3</sub>	OCH <sub>3</sub>		OH	OH		7.19
7		OCH <sub>3</sub>		OH	OCH <sub>3</sub>		OH	OH		7.13
8		OH		OCH <sub>3</sub>	OCH <sub>3</sub>		OH	OH		7.11
9		OH	OH	OH	OCH <sub>3</sub>		OH	OH		6.92
10		OCH <sub>3</sub>	OH	OCH <sub>3</sub>			OH	OH		6.85
11		OCH <sub>3</sub>	OCH <sub>3</sub>	OCH <sub>3</sub>	OCH <sub>3</sub>			OH		6.79
12		OCH <sub>3</sub>		OCH <sub>3</sub>	OH		OH	OH		6.79
13	OCH <sub>3</sub>	OCH <sub>3</sub>		OCH <sub>3</sub>	OCH <sub>3</sub>		OH	OH		6.77
14		OH	OH	OH			OH	OH		6.69
15		OH	OCH <sub>3</sub>	OCH <sub>3</sub>			OH	OH		6.77
16		OH		OCH <sub>3</sub>	OH		OH	OH		6.64
17	OCH <sub>3</sub>	OH		OH	OCH <sub>3</sub>		OH	OH		6.62
18	OCH <sub>3</sub>	OCH <sub>3</sub>	OCH <sub>3</sub>	OCH <sub>3</sub>			OH	OH		6.57
19		OH		OH	OCH <sub>3</sub>		OH	OH		6.55
20	OCH <sub>3</sub>	OCH <sub>3</sub>		OH	OCH <sub>3</sub>		OH	OH		6.55
21		OH	OH	OCH <sub>3</sub>			OH	OH		6.52
22	OCH <sub>3</sub>	OCH <sub>3</sub>	OH	OCH <sub>3</sub>			OH	OH		6.52
23	OCH <sub>3</sub>	OH	OCH <sub>3</sub>	OCH <sub>3</sub>			OH	OH		6.46
24		OH	OCH <sub>3</sub>	OH	OCH <sub>3</sub>			OH		6.39
25		OH	OCH <sub>3</sub>	OCH <sub>3</sub>	OCH <sub>3</sub>			OH		6.27
26	OCH <sub>3</sub>	OH	OH	OCH <sub>3</sub>			OH	OH		6.09
27		OH	OH	OCH <sub>3</sub>	OCH <sub>3</sub>			OH		6.07
28		OH	OH	OH	OCH <sub>3</sub>			OH		5.92
29		OH	OH	OH	OCH <sub>3</sub>		OCH <sub>3</sub>	OH		5.92
30		OH	OCH <sub>3</sub>	OCH <sub>3</sub>				OH		5.85
31		OH	OCH <sub>3</sub>	OH	OCH <sub>3</sub>		OCH <sub>3</sub>	OH		5.35
32		OCH <sub>3</sub>	OH	OCH <sub>3</sub>	OCH <sub>3</sub>		OCH <sub>3</sub>	OH		5.20
33		OH	OCH <sub>3</sub>	OCH <sub>3</sub>			OCH <sub>3</sub>	OH		5.17
34		OH	OCH <sub>3</sub>	OH	OCH <sub>3</sub>			OCH <sub>3</sub>		5.14
35		OH	OH	OH	OCH <sub>3</sub>					5.09
36		OH	OH	OCH <sub>3</sub>	OCH <sub>3</sub>					5.08
37		OH	OCH <sub>3</sub>	OCH <sub>3</sub>	OCH <sub>3</sub>		OCH <sub>3</sub>	OH		4.34
38		OH	OH	OCH <sub>3</sub>	OCH <sub>3</sub>		OCH <sub>3</sub>	OH		3.96
39		OCH <sub>3</sub>	OH	OCH <sub>3</sub>	OCH <sub>3</sub>					3.54
40		OH		OCH <sub>3</sub>		OCH <sub>3</sub>		OCH <sub>3</sub>	OH	3.50
41		OCH <sub>3</sub>		OH						3.00
42		OH		OCH <sub>3</sub>		OCH <sub>3</sub>		OH	OCH <sub>3</sub>	3.00
43				OH						5.78
44				OH						5.64
45			OH							5.28
46				OH						6.46

<sup>a</sup> –log IC<sub>50</sub>: where IC<sub>50</sub> represents the dose of compound in mole required to produce 50% inhibition of Aldose Reductase enzyme.

required to produce 50% ALR2 inhibition (–log IC<sub>50</sub>). The ALR2 inhibitory activity of the selected molecules was determined using a same experimental protocol, and pIC<sub>50</sub> value spanned over a wide range, i.e. 7.55–3.00. The chemical structures of all molecules were sketched using “builder tools” option of “Maestro” program version 9.3 [31], and then their 3D geometries were energy optimized in “LigPrep” program version 2.5 [32] using “OPLS\_2005” force field [33]. The least energy conformers of all molecules were generated employing ‘systematic torsional sampling’ algorithm, and thereafter the ionic states were generated at pH value of 7.0 ± 0.2—a pH value used during ALR2 activity (pIC<sub>50</sub>) determination of 46 studied molecules.

## 2.2. Docking analysis

All molecular docking simulation experiments were performed in “Glide” program version 5.8 [34,35] that performs constrained docking, in which the protein molecule is kept constant while the ligand is allowed to undergo conformational sampling. Glide include three levels of conformational sampling for docking

precisions, i.e. extra precision (XP), standard precision (SP) and high throughput virtual screening (HTVS). Among these three precision levels, XP is the most accurate and produce significantly good conformations as compared to SP and HTVS; however, it is more time consuming. Thus, for the present analysis, Glide-XP was employed for all docking simulations.

For docking simulations, seven crystal structures of ALR2 were downloaded from protein data bank, i.e. 1US0 [36], 1PWM [37], 1Z8A [38], 2PZN [39], 3U2C [40], 1Z3N [41], 1T41 [42]. The downloaded protein structures were devoid of hydrogen atoms, and contain solvent molecules; thus, they needed to be rectified prior to use for docking analysis. All proteins were rectified in “Protein Preparation Wizard” [43], and their rectification included removal of solvent molecules, addition of hydrogen atoms, filling of missing side chains and loops, and completion of ligand bond order. Thereafter, the protein complex was minimized with restricted minimization implemented in “impref”, a sub-procedure of “protein preparation wizard”, and after this minimization, a new complex was within 0.15 Å RMSD (root mean square derivation) for binding pocket residues from a reference crystal structure.

Among the selected proteins, a universal crystal structure that could serve as a representative for ALR2 protein to analyze the interactions of its ligands, was selected based on cross-validation results of all proteins [44]. In the cross docking protocol, the crystal ligands of all selected protein structure were sketched, energy minimized, and their global minimum conformation was generated using 'systematic conformational sampling'. Thereafter, the generated conformation of each crystal ligand was re-docked into the active site of each protein structure. After re-docking, the docked conformation of each crystal ligand was compared with its respective native crystal conformation, and RMSD between these two conformations was determined in terms of all atoms. Finally, an average RMSD value was calculated from the RMSD values of all crystal ligands in each protein system, and a protein describing the lowest value of average RMSD was selected for ligand docking.

For the docking runs, the maximum number of docked conformations was set as ten, and the best docked conformation of each molecule was selected based on docking energy and visual inspection. The visual inspection includes analysis of hydrogen bonding, orientation and position of molecules.

### 2.3. Protein-ligand complex minimization

To remove the unfavourable steric clashes, ligand–protein complexes—obtained from "Glide" docking—were processed using "MM-GBSA" (Molecular Mechanics/Generalized Born Surface Area) calculations in "Prime" (version 3.1) program [45]. For this purpose, the receptor segment of 7 Å around the docked ligand was kept as flexible during complex minimization. In addition to minimization of ligand–protein complex, strain and binding free energy of the ligand was also calculated. The binding free energy ( $\Delta G_{\text{bind}}$ ), calculated with "MM-GBSA", can be formalized as  $\Delta G_{\text{bind}} = \Delta E_{\text{MM}} + \Delta G_{\text{solv}} - T\Delta S$  relationship, where  $\Delta E_{\text{MM}}$ ,  $\Delta G_{\text{solv}}$  and  $-T\Delta S$  are the changes of the gas phase molecular mechanics energy, solvation free energy and conformational entropy upon binding, respectively.  $\Delta E_{\text{MM}}$  includes  $\Delta E_{\text{internal}}$  (bond, angle and dihedral energies),  $\Delta E_{\text{elec}}$  (electrostatic) and  $\Delta E_{\text{vdw}}$  (van der Waals) energy.  $\Delta G_{\text{solv}}$  (solvation energy) is a sum of electrostatic solvation energy (polar contribution),  $\Delta G_{\text{GB}}$ , and the non-electrostatic solvation component (non-polar contribution of surface energy),  $\Delta G_{\text{SA}}$  [46].

### 2.4. Atom-based 3D-QSAR: model generation and validation

In computer assisted drug design, 3D-QSAR term describes the development of a mathematical regression model between 3D structural features of molecules (*i.e.* independent variable denoted as X) and their corresponding biological activity values (dependent variable denoted as Y), with the help of chemometric techniques, *e.g.* Partial Least Square (PLS) analysis. The generated 3D-QSAR model could be used to extract out the vital structural features of molecules required to improve their biological activity, and for the activity prediction of newly designed molecules [47–49].

To develop an atom based 3D-QSAR model, an aligned bundle of all training set molecules was placed into a regular grid of cubes (1 Å × 1 Å × 1 Å). Each cube of the grid is allotted a 0 or 1 "bit value" to account for different types of atom features present in the molecules that occupy these cubes. In this way, binary expression of each training set molecule generates a large dataset of bit values, which was utilized as independent variable, and subsequently correlated with biological activity to develop a 3D-QSAR model. For model generation, "t-value" was set as less than 2, and grid spacing as 1 Å. "PHASE" program [47,48] generates a series of 3D-QSAR models considering progressively more PLS factors, which should not be more than 1/5th of total number of molecules in training set.

The best model was selected based on various statistical parameters including  $Q^2_{\text{test}}$ ,  $R^2_{\text{train}}$  and standard deviation (SD).

The selected model was validated for its prediction ability and reliability. The selected model was validated by performing "Y-randomization" test, leave group out (LGO) cross-validation, and calculating "applicability domain (APD)" [50,51] and statistical parameters as suggested in [52].

"Applicability domain" was calculated to describe the reliability of generated model to predict new molecules. For "APD" calculation, similarity measurements were calculated based on Euclidean distances between all pairs of training and test set compounds separately [50,51]. Initially, average ( $\mu$ ) of all Euclidean distances between the training set compounds was calculated, and thereafter new average  $\langle d \rangle$  and standard deviation ( $\sigma$ ) of training set molecules with distances lower than the value of  $\mu$  were computed. Z is an empirical cutoff with default value of 0.5.

$$\text{APD} = \langle d \rangle + \sigma Z$$

To evaluate the sensitivity of the generated models to chance correlations 'leave many out (LMO)' parameter was calculated. In LMP cross-validation, 'n' molecules were omitted from the data set, and remaining molecules were utilized to develop new model, which was further used to predict the omitted 'n' molecules. The same process was continuously repeated until each molecule is omitted and predicted once.

"Y-randomization" test was employed to determine the regression quality of generated model. For this test, the activity data of training set molecules was scrambled, and new training sets were generated, which were thereafter utilized to develop new QSAR models and determine new  $R^2_{\text{train}}$  values [50,51]. The average of  $R^2_{\text{train}}$  obtained from scrambled (new) training sets, denoted by  $R^2_{\text{scramble}}$ , was determined that must describe low value as compared to original  $R^2_{\text{train}}$  value of the selected model, if not, then the selected model would be meaningless and generated by chance.

In addition to these validation parameters, professor Golbraikh and Tropsha have described a criteria of few statistical parameters that the developed QSAR model should satisfy order to get considered as a reliable model. A good QSAR model should always have coefficient of correlation close to the ideal model ( $R^2_{\text{train}} = 1$ ) for having high predictive reliability. In addition to original  $R^2_{\text{train}}$  of the generated model, the correlation coefficients of the regression lines passing through the origin, *i.e.*  $R_o^2$  (predicted versus observed activities) and  $R'_o^2$  (observed versus predicted activities) should also be close to  $R^2_{\text{train}}$ . Moreover,  $[(R^2 - R_o^2)/R^2]$  and  $[R^2 - R'_o^2]/R^2$  should be less than 0.1, and the corresponding 'slopes' of  $R_o^2$  and  $R'_o^2$  regression lines, *i.e.* k and k' should be between 0.85 and 1.15 ( $0.85 \leq k, k' \leq 1.15$ ) [52].

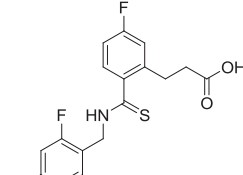
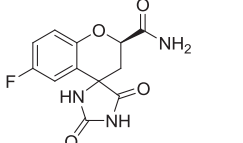
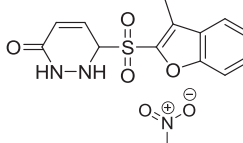
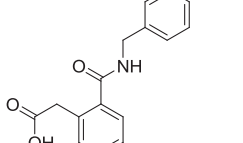
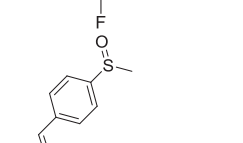
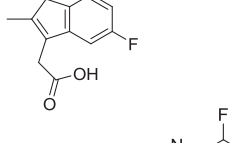
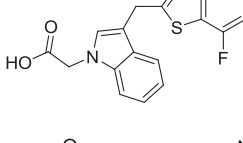
## 2.5. Chemical synthesis

### 2.5.1. Material required

All chemicals required for synthetic protocol were purchased from Sigma Aldrich, and they were >99% pure as certified by manufacturer, thus used without any further purification. At each step, the completion of chemical reaction was monitored with thin layer chromatography {DC-Alufolien (20 cm × 20 cm) Kieselgel 60 F254 chromatic plates} using hexane:ethyl acetate (6:4) as TLC development solvent system. The products of all chemicals reactions were purified by either eluting on silica columns or re-crystallization from appropriate solvent. Melting point of each compound was noted on Labtronics digital automatic melting point apparatus. The characterization of all compounds was performed based on their respective spectral data. Infra red (IR) spectra of compounds was recorded on Bruker® (Alpha E) FT-IR spectrometer, mass spectra on

**Table 2**

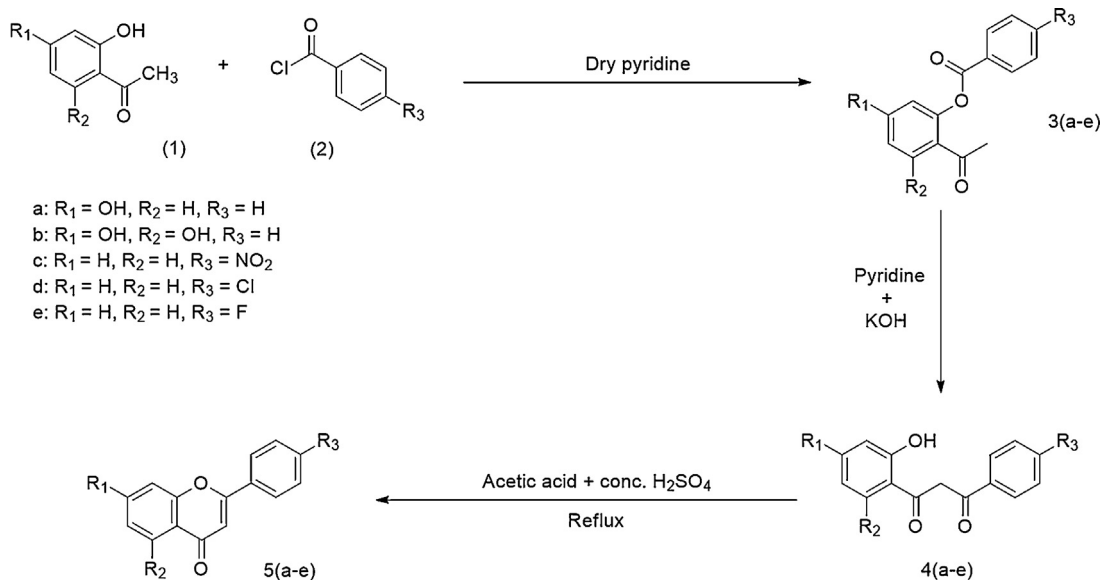
Results of cross-docking experiments for the selected seven crystal structures of ALR2.

Protein Data Bank Codes	Ligand from PDB	Ligand structure	Protein structures						
			1US0	1PWM	1Z8A	2PZN	3UZC	1Z3N	1T41
1US0			0.26	6.50	3.80	2.30	4.80	2.40	3.50
1PWM			3.68	0.40	0.93	1.61	1.41	1.00	0.86
1Z8A			0.64	7.10	4.67	3.34	6.20	0.71	1.24
2PZN			0.67	7.10	4.38	0.12	6.03	0.82	0.25
3UZC			1.38	6.42	2.90	1.67	0.25	3.70	4.10
1Z3N			0.41	4.90	4.95	0.49	5.70	0.35	0.37
1T41			1.87	6.50	5.04	0.59	9.50	1.01	0.20
Average RMSD (Å)			<b>1.27</b>	5.56	3.81	1.44	4.84	1.42	1.50

<sup>a</sup> Root Mean Square Deviations between ligand crystal structure and redocked structure.

Bold depicts the lowest RMSD in cross-docking that was used to select the corresponding protein 1US0.

RMSD between crystal ligand and re-docked structure (Å)

**Scheme 1.** Synthetic protocol for the synthesis of designed molecules.

Waters® Q-TOF micromass (LC–MS) using ESI (+) mode, and proton (<sup>1</sup>H) NMR spectra on Bruker® Advance-II 400 MHz NMR spectrometer using deuterated chloroform (CDCl<sub>3</sub>-d<sub>6</sub>) or dimethylsulfoxide (DMSO-d<sub>6</sub>) as solvent.

### 2.5.2. Chemical reactions

The complete synthetic protocol for compounds 5a–e is displayed in **Scheme 1**. In the first step of synthetic protocol, substituted o-benzoyloxyacetophenones (3a–e) were synthesized from the chemical reaction of substituted o-hydroxyacetophenone (1, 0.1 mol) with substituted benzoyl chlorides of choice (2, 0.15 mol) in the presence of dry pyridine as solvent. The hot reaction mixture, due to spontaneous evolvement of heat, was allowed to cool down and attain room temperature. Then, the cool mixture was poured, with constant stirring, into 3% hydrochloric acid containing crushed ice that results in the precipitation of solid residue. This solid residue was filtered, washed with methanol followed by water, and air-dried. The re-crystallization of this solid from methanol results in white precipitates of pure substituted o-benzoyloxyacetophenones (3a–e).

The second step involved the synthesis of substituted o-hydroxy-di-benzoylmethane molecules (4a–e) from intermediate compounds (3a–e), in the presence of dry pyridine. The solution of compound 3a–e in dry pyridine was heated to 50 °C, and 7 g of hot pulverized potassium hydroxide (85%) was added to it. The mixture was mechanically stirred for 15 min that resulted in the gradual appearance of yellow precipitates of potassium salt of substituted o-hydroxy di-benzoylmethane molecules. The reaction mixture was allowed to achieve room temperature, and thereafter acidified with 100 ml of 10% acetic acid to desalt the compounds. The pure diketone compounds (4a–e) were obtained as light-yellow coloured solid that were filtered and air-dried.

Furthermore, in the third step of synthetic protocol, diketone molecules (4a–e) were refluxed (1 h) on water bath in the presence of glacial acetic acid and conc. sulphuric acid, to achieve cyclized products. Upon the completion of chemical reaction, monitored by TLC, the reaction mixture was poured onto crushed ice with vigorous stirring that resulted in the precipitation of crude flavone product [53,54]. The crude product was filtered, washed with water to remove acid traces and air-dried. The crude solid was eluted on

silica column using hexane:ethyl acetate (6:4) as solvent system, to obtain pure flavone compounds (5a–e).

### 2.6. Biological evaluation

#### 2.6.1. Material required

To perform ALR2 inhibitory activity assay, following chemicals and materials were procured and used for study. DL-glyceraldehyde (Sigma Aldrich), NADPH and 2-mercaptoethanol (Himedia Laboratories Pvt. Ltd., Mumbai), epalrestat (Microlabs Ltd.), sodium carbonate, dipotassium hydrogen orthophosphate, ammonium sulphate, lithium sulphate and sodium hydroxide (Loba Chemicals Pvt. Ltd., Mumbai). All required solutions for study were freshly prepared, and goat eyes were obtained from a local abattoir soon after slaughtering.

#### 2.6.2. Assay method

The eye lenses of a freshly slaughtered goat were surgically removed, washed with cold distilled water, and homogenized in cold water (distilled) containing 10 mM 2-mercaptoethanol (1:3 w/v). The homogenate was centrifuged (10,000 rpm) for 30 min at 4 °C, and thereafter, the supernatant liquid was saturated by adding 40% ammonium sulphate. The saturated solution was filtered, and the filtrate was again centrifuged (10,000 rpm) for 30 min at 4 °C to get a clear lens solution containing ALR2 enzyme which was (supernatant) utilized for ALR2 enzyme assay [55,56].

The assay reaction mixture contained 1 ml of supernatant (ALR2), 1 ml of 0.0067 M phosphate buffer containing 0.104 mM NADPH, 10 mM glyceraldehyde, 0.4 M LiSO<sub>4</sub> and 1 ml of different concentrations of inhibitors (2.5 µg/ml, 5 µg/ml, 10 µg/ml, 20 µg/ml, 40 µg/ml). The enzyme reaction starts upon the addition of a substrate molecule, i.e. glyceraldehyde (10 mM), and the absorbance of assay reaction mixture was recorded for 3 min on a UV spectrophotometer at 340 nm. The enzyme inhibitory activity of each compound was calculated based on reduction in absorbance of reaction mixture due to decreased enzymatic oxidation of NADPH to NADP<sup>+</sup> by ALR2. The activity of each compound at different concentrations was calculated using following formula, where  $\Delta A$

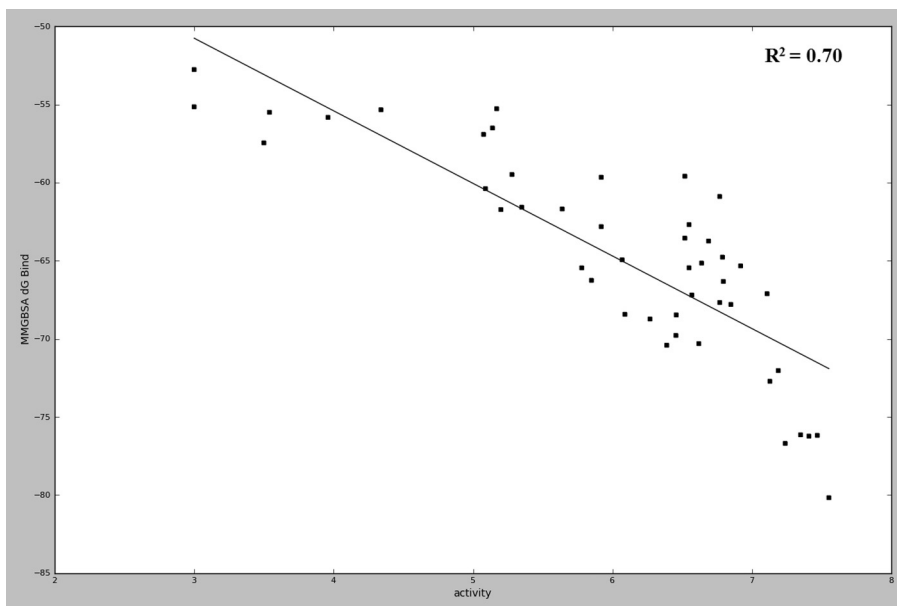


**Fig. 4.** The correlation graph between experimental activities of molecules and free energy of binding calculated in "MM-GBSA".

test/min is the rate of change of absorbance per minute for test sample [55,56].

Activity U/ml(units per millilitre)

$$= \frac{\Delta A \text{ test/ min} \times \text{Total volume of assay mixture}}{(6.2 \mu\text{M}, \text{extinction coefficient of NADPH at } 340 \text{ nm}) \times \text{Volume of enzyme taken for analysis}}$$

The percentage inhibition of all compounds was calculated by considering 100% ALR2 activity in the absence of inhibitor. The concentration of each test compound giving 50% inhibition ( $IC_{50}$ ) was determined by plotting log concentration of test compounds versus percentage inhibition.

### 3. Results and discussion

3D-QSAR is a ligand based drug design method usually implemented for lead optimization. This method basically depends upon the alignment of congener molecules, and subsequent comparison of their substitution pattern or functional moieties. The molecular alignment of 46 studied flavone derivatives was achieved by the docking analysis coupled with "MM-GBSA" ligand–protein complex refinement, and thereafter the aligned bundle was utilized for the generation of 3D-QSAR models. The selected 3D-QSAR model was employed for the designing of new flavonoid congeners, which were duly synthesized and evaluated for their ALR2 inhibitory activity *in vitro*.

#### 3.1. Cross-docking experiment: validation of active sites and the selection of a reliable protein crystal structure for docking simulations

Since no experimental 3D structure of protein ALR2 co-crystallized with flavonoid molecule has been reported in the protein data bank, the most reliable or appropriate crystal structure was selected based on cross-docking experiment [44]. In the literature, several crystal structures of ALR2 co-crystallized with small molecule inhibitors have been reported. Thus, to narrow down this limit, top seven crystal structures were considered for the analysis based on their resolution and crystal ligand diversity.

The selected crystal structures include 1US0, 1PWM, 1Z8A, 2PZN, 3U2C, 1Z3N and 1T41. The cross-docking experiment, using "XP mode of Glide" docking program [34,35], was performed with all

seven crystal structures, and the results showed the least average RMSD value of  $1.27 \text{ \AA}$  for protein structure 1US0 (Table 2). This analysis showed that the crystal structure 1US0 is capable of reproducing the native crystal conformations of re-docked seven crystal ligands with minimum all atom deviation as compared to other protein crystal structures. Therefore, it was hypothesized that in the absence of 3D structure co-crystallized with flavone molecules, 1US0 would produce precise docking poses of the studied flavone derivatives since it can significantly reproduce the native crystal structures of the experimentally determined seven crystal ligands.

#### 3.2. Molecular alignment: docking analysis and MM-GBSA ligand–protein complex refinement

3D-QSAR analysis is alignment sensitive method, and appropriate alignment of congeneric molecules is prerequisite for this analysis. Therefore, docking based alignment was derived using

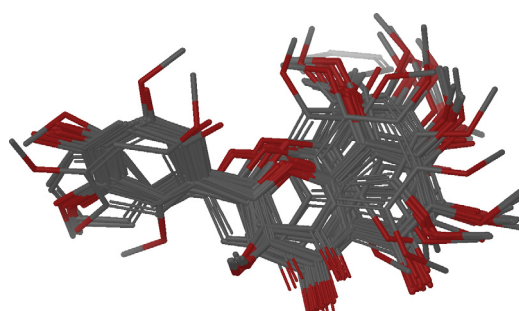


**Fig. 5.** Alignment bundle of ALR2 inhibitors used for atom-based 3D-QSAR.

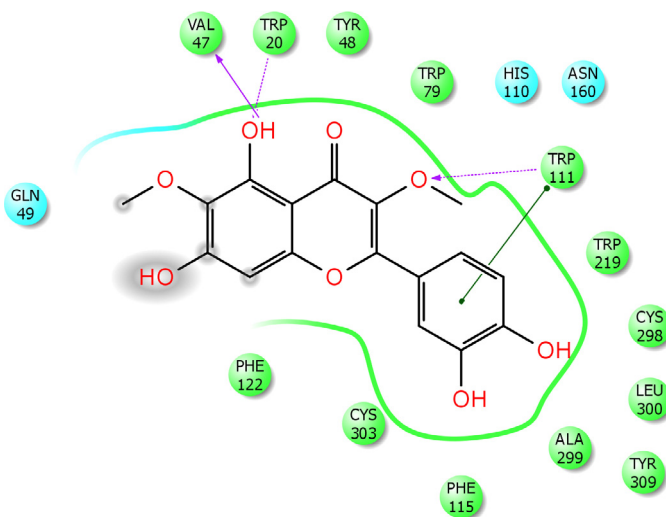


**Fig. 6.** 2D representation of the docking interactions of molecule 1 within the active site of protein ALR2 (PDB ID 1USO).

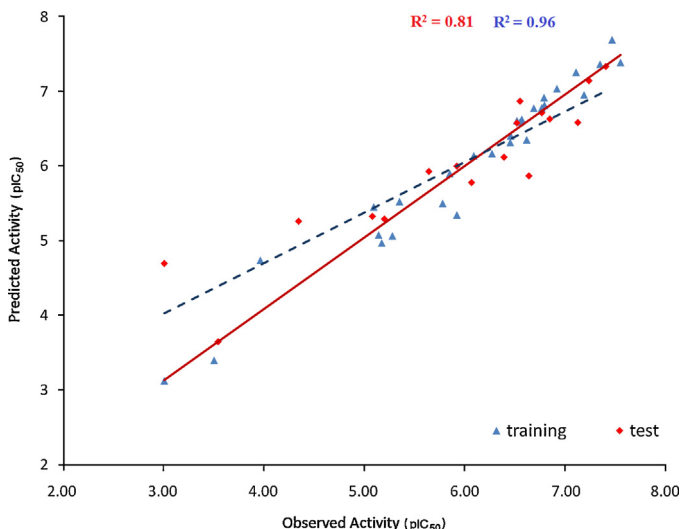


**Fig. 7.** The correlation graph between experimental and predicted activities of training and test set molecules from selected atom-based 3D-QSAR model (QSAR<sub>4</sub>).

protein crystal structure 1USO, which is selected from cross-docking validation protocol. For this purpose, 46 studied molecules were docked into the active site of 1USO using “XP mode of Glide” docking program. The docked poses of all molecules were analyzed, and the best pose of each molecule was subsequently selected based on Glide score and manual inspection [57].

“Glide” docking program perform constrained docking of ligands, in which only ligand molecule is allowed to undergo conformational changes while the protein molecule is kept con-

stant. Contrary to this, protein molecules, at the molecular level, are highly flexible and their active site amino acid residues undergo conformational changes upon ligand binding. Thus, in the constrained docking of “Glide” program, crucial conformational changes in the active site of protein would remain intact that could assist the good complementary fit of docking ligand with protein [44,57–59]. In the light of this, “Glide” docking obtained protein–ligand complexes were refined in the “Prime” program using “MM-GBSA” method. Additionally, “MM-GBSA” calculates binding free energy of ligands that can be correlated with the activity to check the goodness of refined conformations. After “MM-GBSA” refinement of protein–ligand complexes, the correlation between the activity and the free energy of binding was observed to be 0.70 ( $R^2$ ) which described the significant binding conformations of the studied molecules (Fig. 4). Thereafter, the studied molecules were isolated from “MM-GBSA” refined ligand–protein complexes, and the obtained molecular alignment (Fig. 5) was utilized for the generation of 3D-QSAR models. The “MM-GBSA” refined pose of the highest active molecule 1 within the active site of 1USO is displayed in Fig. 6. In this figure, molecule 1 showed a network of hydrogen bonding interactions enabling its efficient binding within the active site of protein ALR2. In this molecule, the OH group present at the 5<sup>th</sup> position showed two hydrogen bonding interactions with Val47 and Trp20, the ‘O’ of the methoxy group at 3<sup>rd</sup> position showed the hydrogen bond with Trp111 and the phenyl ring substituted at the 2<sup>nd</sup> position showed the π–π interactions with Trp111.

### 3.3. Generation of the atom-based 3D-QSAR model and its validation

The aligned bundle of studied 46 flavones was imported into “PHASE” program for the generation of 3D-QSAR models. “PHASE” includes two options for the generation of 3D-QSAR models named as atom- and pharmacophore based [49,50]. The difference between these two is whether all atoms or only the pharmacophore sites of the molecules are considered. The choice of which type of model to create depends largely on whether or not the training set molecules are sufficiently rigid and congeneric. If the structure contains a relatively small number of rotatable bonds and some common structural framework, then an atom-based model may work quite well. Our data set is congeneric, i.e. flavone derivatives; thus atom-based approach of “PHASE” was employed to generate 3D-QSAR model. The total data set was randomly divided into training and test set, of 29 and 17 molecules, respectively, ensuring the uniform distribution of biological activity and structural variation into both sets. The selected training set was then utilized for the generation of an atom based 3D-QSAR models. The best model was selected corresponding to PLS factor 4 based on the highest value of  $Q^2_{\text{test}}$  (0.81). The selected model also exhibited high values of  $R^2_{\text{train}}$  (0.96),  $F$  (130.90) and low SD (0.26). The statistical results of the selected 3D-QSAR model (QSAR<sub>4</sub>) are depicted in Table 3, and the predicted activity of training set molecules using this model is mentioned in Table 4. The correlation graph between the experimental

**Table 3**  
Statistical results of the generated atom-based 3D-QSAR models.

Model	PLS factor	SD	$R^2_{\text{train}}$	F-value	RSME	$Q^2_{\text{test}}$	Pearson-r
QSAR <sub>1</sub>	1	0.57	0.76	82.20	0.71	0.67	0.87
QSAR <sub>2</sub>	2	0.39	0.89	105.10	0.63	0.74	0.89
QSAR <sub>3</sub>	3	0.33	0.93	105.60	0.57	0.79	0.92
<b>QSAR<sub>4</sub></b>	<b>4</b>	<b>0.26</b>	<b>0.96</b>	<b>130.90</b>	<b>0.55</b>	<b>0.81</b>	<b>0.92</b>
QSAR <sub>5</sub>	5	0.23	0.97	137.70	0.56	0.78	0.91

SD, Standard deviation;  $R^2_{\text{train}}$ , coefficient of determination for training set molecules; F-value, Fisher test; RMSE, root mean squared error;  $Q^2_{\text{test}}$ , coefficient of determination for test set molecules; Pearson-r, Pearson coefficient of correlation for test set molecules.  
Bold selection depicts the selected 3D-QSAR model.

**Table 4**

Dataset of molecules used for generation of atom based 3D-QSAR model and their corresponding predicted activity values based on the selected model (QSAR<sub>4</sub>).

Sr. No.	Biological Activity (pIC <sub>50</sub> )	
	Experimental	Predicted
1	7.55	7.38
2	7.47	7.69
3 <sup>a</sup>	7.41	7.33
4	7.35	7.36
5 <sup>a</sup>	7.24	7.14
6	7.19	6.95
7 <sup>a</sup>	7.13	6.58
8	7.11	7.25
9	6.92	7.03
10 <sup>a</sup>	6.85	6.63
11	6.79	6.82
12	6.79	6.91
13	6.77	6.78
14	6.69	6.77
15 <sup>a</sup>	6.77	6.72
16 <sup>a</sup>	6.64	5.87
17	6.62	6.35
18	6.57	6.62
19 <sup>a</sup>	6.55	6.87
20	6.55	6.59
21 <sup>a</sup>	6.52	6.58
22	6.52	6.61
23	6.46	6.40
24 <sup>a</sup>	6.39	6.12
25	6.27	6.17
26	6.09	6.14
27 <sup>a</sup>	6.07	5.78
28 <sup>a</sup>	5.92	5.99
29	5.92	5.35
30	5.85	5.90
31	5.35	5.52
32 <sup>a</sup>	5.20	5.29
33	5.17	4.97
34	5.14	5.07
35	5.09	5.45
36 <sup>a</sup>	5.08	5.32
37 <sup>a</sup>	4.34	5.26
38	3.96	4.74
39 <sup>a</sup>	3.54	3.65
40	3.50	3.40
41	3.00	3.12
42 <sup>a</sup>	3.00	4.70
43	5.78	5.5
44 <sup>a</sup>	5.64	5.93
45	5.28	5.06
46	6.46	6.13

<sup>a</sup> Test set molecules.

and predicted activities of training set molecules is displayed in Fig. 7.

The external validation of the selected model was performed by calculating Pearson-r for the test set molecules, which displayed significantly good value of 0.92. The correlation graph between

experimental and predicted activities of the test set molecules is displayed in Fig. 7. Further, the external predictive reliability of the selected model QSAR<sub>4</sub> was also checked by calculating  $k$  (1.01),  $k'$  (0.99),  $R_0^2$  (0.98) and  $R'_0$  (0.98), which all displayed acceptable values [52]. To check the predictive reliability of the selected model for new molecules, "APD" calculation was done, in which the similarity distances of test set molecules were well within the threshold range of model, i.e. "APD" of training set (Table 5). Further, the cross validated parameter i.e. 'leave group out' was calculated that showed a value of  $R_{CV}^2$  i.e. 0.65 depicting good predictive power of the generated model. The robustness of the selected model was analyzed by performing "Y-randomization" test, which displayed lower value of  $R_{scramble}^2$  (0.88) as compared to the original value of  $R_{train}^2$  (0.96). Finally, the contour plots of different properties including hydrophobic, hydrogen bonding donor and electron withdrawing property were generated for the selected model QSAR<sub>4</sub> (Fig. 8).

### 3.4. Designing of congener molecules: synthesis and biological evaluation

The contour maps were analyzed and the information revealed from them was duly utilized for the designing of new five congener molecules keeping in mind about their synthetic possibility. In Fig. 8A, the Hydrogen Bond Donor (HBD) substitution favourable blue contours are present close to the 7th position of the flavone ring while unfavourable red contours are present at the 5th position of the same ring. Contrary to this, in the docking simulation (Fig. 6), the OH present at the 5th position of the highest active molecule displayed H-bonding interactions. Moreover, the hydrophobic unfavourable red contours are also located near to the 4'-position of the highest active molecule (Fig. 8B). Thus, two molecules, 5a and 5b, were designed based on these observations. In both molecules, 4' position was kept un-substituted, and for molecule 5a, only 7th position was substituted with OH group while for molecule 5b, 7th and 5th, both positions were substituted with OH groups. In Fig. 8C, the electron withdrawing atoms favourable blue contours are located near to the 4' (*para*) position of the highest active molecule, thus based on synthetic possibility, three molecules were designed substituting with electron withdrawing atom bearing groups at this positions, i.e. NO<sub>2</sub>, Cl and F (Table 6). These designed five molecules that qualified the APD (Table 6) were duly synthesized as per the synthetic protocol described in Scheme 1. After synthesis, these molecules were tested for their biological activity against ALR2, and all molecules displayed good micromole activity ( $IC_{50} < 22 \mu M$ ) (Table 6) which are within one log unit of their predicted activity. The graph displaying the predicted and experimental activities of the designed molecules is mentioned in Fig. 9.

The docking study of the highest active compound, i.e. 5d with hydrophobic atoms, i.e. Cl at the para position of ring B was carried out. During docking analysis the ring B substituted with Cl atom

**Table 5**

Applicability domain for test set molecules of atom-based 3D-QSAR model.

Compound	Distance (APD = 3.359)	Compound	Distance (APD = 3.359)
3	1.732	24	2.000
5	2.236	27	1.732
7	2.449	28	1.732
10	2.236	32	2.449
15	1.732	36	2.000
16	2.449	37	2.000
19	2.236	39	2.828
21	2.236	42	1.732
44	1.414		

**Table 6**

Molecular structures, APD values, and predicted and experimental activities of the designed ALR2 inhibitors.

Compound code	Molecular structure	APD (3.359)	pIC <sub>50</sub> <sup>a</sup>		Exp. IC <sub>50</sub> ( $\mu$ M)
			Predicted	Experimental	
5a		2.24	5.08	4.81	15.60
5b		2.24	5.21	4.67	21.60
5c		2.45	5.47	4.99	10.10
5d		2.45	4.50	5.27	5.40
5e		2.83	4.56	5.00	10.00
Standard	Epalrestat	–	–	7.14	0.07

<sup>a</sup> –log IC<sub>50</sub>; where IC<sub>50</sub> represents the dose of compound in mole required to produce 50% inhibition of Aldose Reductase enzyme.

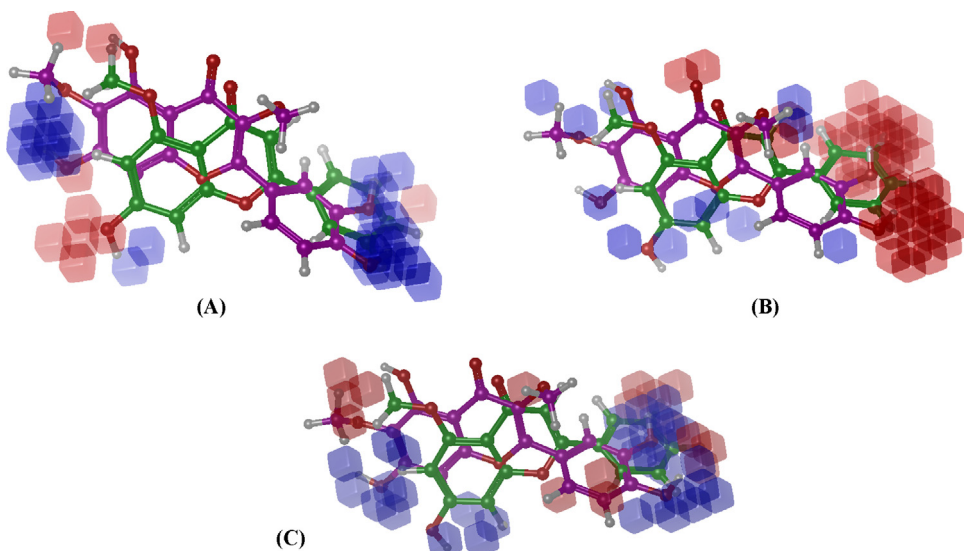


**Fig. 8.** Contour plots for different properties corresponding to QSAR<sub>4</sub> model: Hydrogen bond donor (A), hydrophobic (B), electron withdrawing (C). In all plots the highest active molecule 1 (purple) and least active molecule 41 (green) are displayed in background. (For interpretation of the references to colour in this figure legend, the reader is referred to the web version of this article.)

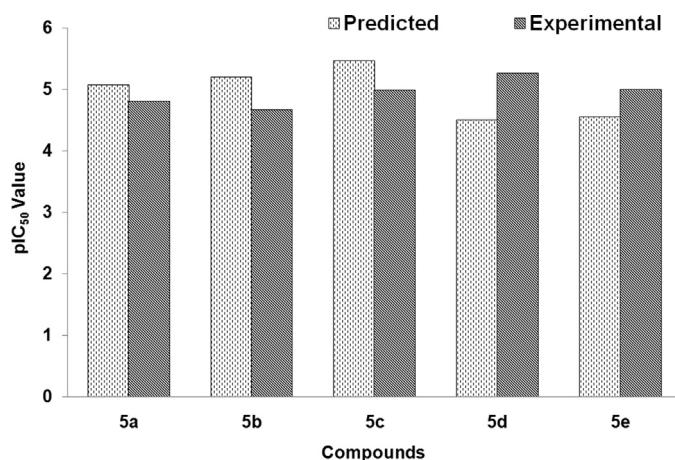


**Fig. 9.** The graphical representation of the experimental and predicted activity of compounds (5a–e).

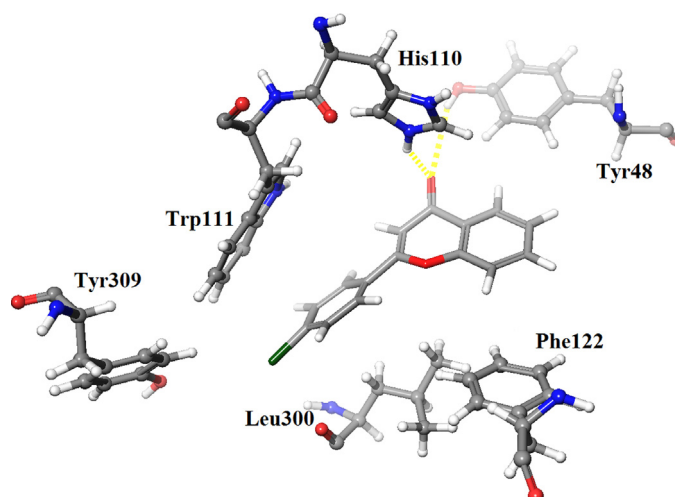


**Fig. 10.** The docking interactions of highest active molecule 5d within the active site of protein ALR2 (PDB 1US0).

was found to interact with hydrophobic pocket of ALR2 lined by Trp111, Phe122 and Leu300 amino acid residues. Additionally, the 'O' of carbonyl group of flavone ring forms hydrogen bonding with His110 and Tyr48 amino acids ([Fig. 10](#)).

#### 4. Conclusions

A highly predictive and statistically validated 3D-QSAR model (QSAR<sub>4</sub>) was developed for 46 studied flavonoid inhibitors of ALR2, and subsequently utilized for the designing of new congener molecules. 3D-QSAR model was developed using "Prime MM-GBSA" refined alignment of "Glide-XP" docking poses of all studied molecules. The selected model showed high internal and external validation, reliability in terms of Pearson-r, "APD", "Y-randomization",  $k$ ,  $k'$ ,  $R_0^2$  and  $R'_0{}^2$  values. The contour plots of the different properties obtained from the selected model helped to extract out the essential structural requirements of the flavonoid molecules that are required for ALR2 activity. Furthermore, using this revealed information; five new congener molecules were designed and duly synthesized. All five molecules showed good in vitro inhibitory activity (<22  $\mu\text{M}$ ) against ALR2, and consequently they could be employed for the management of diabetic complications.

#### Acknowledgements

The authors thank Dr. Ravikumar Muttineni (Application Scientist), Er. Anirban Banerjee (IT Consultant), and Mr. Raghu Rangaswamy from Schrödinger, Bangalore, for their constant scientific and technical support to handle Schrödinger software and work smoothly. Bhawna Vyas and Malkeet Singh acknowledges Indian Council of Medical Research (ICMR), New Delhi, for providing Senior Research Fellowship (SRF); Grant No. 45/15/2011/BIF/BMS and 45/3/2012-BMS/BIF, respectively.

## Appendix A. Supplementary data

Supplementary data associated with this article can be found, in the online version, at <http://dx.doi.org/10.1016/j.jmgm.2015.03.005>

## References

- [1] Data Accessed From Official Diabetes Webpage of WHO <http://www.who.int/mediacentre/factsheets/fs312/en/on> October 19, 2014.
- [2] The Diabetes Control and Complications Trial Research Group, The effect of intensive treatment of diabetes on the development and progression of long-term complications in insulin-dependent diabetes mellitus, *N. Engl. J. Med.* 329 (1993) 977–986.
- [3] UK Prospective Diabetes Study (UKPDS) Group, Intensive blood-glucose control with sulphonylureas or insulin compared with conventional treatment and risk of complications in patients with type 2 diabetes (UKPDS 33), *Lancet* 352 (1998) 837–853.
- [4] P.F. Kador, W.G. Robison, J.H. Kinoshita, The pharmacology of aldose reductase inhibitors, *Annu. Rev. Pharmacol. Toxicol.* 25 (1985) 691–714.
- [5] B.S. Szwergold, F. Kappler, T.R. Brown, Identification of fructose 3-phosphate in the lens of diabetic rats, *Science* 247 (1990) 451–454.
- [6] A.M. Gonzalez, M. Sochor, J.S. Hothersall, P. McLean, Effect of aldose reductase inhibitor (sorbinil) on integration of polyol pathway, pentose phosphate pathway, and glycolytic route in diabetic rat lens, *Diabetes* 35 (1986) 1200–1205.
- [7] K.J. WellsKnecht, E. Brinkmann, M.C. Wells-Knecht, J.E. Litchfield, M.U. Ahmed, S. Reddy, D.V. Zyzak, S.R. Thorpe, J.W. Baynes, New biomarkers of Maillard reaction damage to proteins, *Nephrol. Dial. Transpl.* 11 (1996) 41–47.
- [8] W.G. Robinson Jr., P.F. Kador, J.H. Kinoshita, Retinal capillaries: basement membrane thickening by galactosemia prevented with aldose reductase inhibitor, *Science* 221 (1983) 1177–1179.
- [9] R.L. Engerman, Pathogenesis of diabetic retinopathy, *Diabetes* 38 (1989) 203–1206.
- [10] R.J. Young, D.J. Ewing, B.F. Clarke, A controlled trial of sorbinil, an aldose reductase inhibitor, in chronic painful diabetic neuropathy, *Diabetes* 32 (1983) 938–942.
- [11] M. Dunlop, Aldose reductase and the role of the polyol pathway in diabetic nephropathy, *Kidney Int.* 58 (2000) S3–S12.
- [12] S.D. Varma, J.H. Kinoshita, Inhibition of lens aldose reductase by flavonoids – their possible role in the prevention of diabetic cataracts, *Biochem. Pharmacol.* 25 (1976) 2505–2513.
- [13] A. Seyoum, K. Asres, F.K. El-Fiky, Structure–radical scavenging activity relationships of flavonoids, *Phytochemistry* 67 (2006) 2058–2070.
- [14] B.H. Havsteen, The biochemistry and medical significance of the flavonoids, *Pharmacol. Ther.* 96 (2002) 67–202.
- [15] Y.J. Moon, X. Wang, M.E. Morris, Dietary flavonoids: effects on xenobiotic and carcinogen metabolism, *Toxicol. In Vitro* 20 (2006) 187–210.
- [16] W. Xie, W. Wang, H. Su, D. Xing, Y. Pan, L. Du, Effect of ethanolic extracts of *Ananas comosus* L. leaves on insulin sensitivity in rats and HepG2, *Biochem. Physiol. C: Toxicol. Pharmacol.* 143 (2006) 429–435.
- [17] A.G. Mercader, P.R. Duchowicz, F.M. Fernandez, E.A. Castro, D.O. Bennardi, J.C. Autino, G.P. Romanelli, QSAR prediction of inhibition of aldose reductase for flavonoids, *Bioorg. Med. Chem.* 16 (2008) 7470–7476.
- [18] R. Sheng, X. Lin, J. Zhang, K.S. Chol, W. Huang, B. Yang, Q. He, Y. Hu, Design, synthesis and evaluation of flavonoid derivatives as potent AChE inhibitors, *Bioorg. Med. Chem.* 17 (2009) 6692–6698.
- [19] M.K. Kim, Y. Chong, Towards selective inhibitors of Janus kinase 3: identification of a novel structural variation between Janus kinases 2 and 3, *Bull. Korean Chem. Soc.* 33 (2012) 4207–4210.
- [20] M. Shichijo, N. Yamamoto, H. Tsujishita, M. Kimata, H. Nagai, T. Kokubo, Inhibition of syk activity and degranulation of human mast cells by flavonoids, *Biol. Pharm. Bull.* 12 (2003) 1685–1690.
- [21] N. Cotelle, Role of flavonoids in oxidative stress, *Curr. Top. Med. Chem.* 1 (2001) 569–590.
- [22] Y.S. Prabhakar, M.K. Gupta, N. Roy, Y. Venkateswarlu, A high dimensional QSAR study on the aldose reductase inhibitory activity of some flavones: topological descriptors in modeling the activity, *J. Chem. Inf. Model.* 46 (2006) 86–92.
- [23] H. Liu, S. Liu, L. Qin, L. Mo, CoMFA and CoMSIA analysis of 2,4-thiazolidinediones derivatives as aldose reductase inhibitors, *J. Mol. Model.* 15 (2009) 837–845.
- [24] T.S. Aggarwal, T.R. Bhardwaj, M. Kumar, 3D-QSAR studies on a series of 5-arylidine-2,4-thiazolidinediones as aldose reductase inhibitors: a self-organizing molecular field analysis approach, *Med. Chem.* 6 (2010) 30–36.
- [25] M. Fernandez, J. Caballero, A.M. Helguera, E.A. Castro, M.P. Gonzalez, Quantitative structure–activity relationship to predict differential inhibition of aldose reductase by flavonoid compounds, *Bioorg. Med. Chem.* 13 (2005) 3269–3277.
- [26] J.C. Patra, O. Singh, Artificial neural networks-based approach to design ARIs using QSAR for diabetes mellitus, *J. Comput. Chem.* 30 (2009) 2494–2508.
- [27] L. Hu, G. Chen, R.M. Chau, A neural networks-based drug discovery approach and its application for designing aldose reductase inhibitors, *J. Mol. Graph. Model.* 24 (2006) 244–253.
- [28] A. Stefanic-Petek, A. Kravacic, T. Solmajer, QSAR of flavonoids: 4. Differential inhibition of aldose reductase and p56ck protein tyrosine kinase, *Croat. Chem. Acta* 75 (2002) 517–529.
- [29] M. Fernández, J. Caballero, A.M. Helguera, E.A. Castro, M.P. González, Quantitative structure–activity relationship to predict differential inhibition of aldose reductase by flavonoid compounds, *Bioorg. Med. Chem.* 13 (2005) 3269–3277.
- [30] J. Caballero, 3D-QSAR (CoMFA and CoMSIA) and pharmacophore (GALAHAD) studies on the differential inhibition of aldose reductase by flavonoid compounds, *J. Mol. Graph. Model.* 29 (2010) 363–371.
- [31] Maestro, Version 9.3, Schrödinger, LLC, New York, NY, 2012.
- [32] LigPrep, Version 2.5, Schrödinger, LLC, New York, NY, 2012.
- [33] D. Shivakumar, J. Williams, Y. Wu, W. Damm, J. Shelley, W. Sherman, Prediction of absolute solvation free energies using molecular dynamics free energy perturbation and the OPLS force field, *J. Chem. Theory Comput.* 6 (2010) 1509–1519.
- [34] R.A. Friesner, J. Banks, R.B. Murphy, T.A. Halgren, J.J. Klicic, D.T. Mainz, M.P. Repasky, E.H. Knoll, D.E. Shaw, M. Shelley, J.K. Perry, P. Francis, P.S. Shenkin, Glide a new approach for rapid, accurate docking and scoring. 1. Method and assessment of docking accuracy, *J. Med. Chem.* 47 (2004) 1739–1749.
- [35] Glide, Version 5.8, Schrödinger, LLC, New York, NY, 2012.
- [36] E.I. Howard, R. Sanishvili, R.E. Cachau, A. Mitschler, B. Chevrier, P. Barth, V. Lamour, M. Van Zandt, E. Sibley, C. Bon, D. Moras, S.T.R. Schneider, A. Joachimiak, A. Podjarny, Ultrahigh resolution drug design I: details of interactions in human aldose reductase–inhibitor complex at 0.6 Å, *Proteins* 55 (2004) 792–804.
- [37] O. El-Kabbani, C. Darmanin, T.R. Schneider, I. Hazemann, F. Ruiz, M. Oka, A. Joachimiak, C. Schulze-Briese, T. Tomizaki, A. Mitschler, A. Podjarny, Ultrahigh resolution drug design II, atomic resolution structures of human aldose reductase holoenzyme complexed with Fidarestat and Minalrestat: implications for the binding of cyclic imide inhibitors, *Proteins* 55 (2004) 805–813.
- [38] H. Steuber, M. Zentgraf, A. Podjarny, A. Heine, G. Klebe, High-resolution crystal structure of aldose reductase complexed with the novel sulfonyl-pyridazinone inhibitor exhibiting an alternative active site anchoring group, *J. Mol. Biol.* 356 (2006) 45–56.
- [39] F. Ruiz, I. Hazemann, C. Darmanin, A. Mitschler, M. Van Zandt, A. Joachimiak, O. El-Kabbani, A. Podjarny, doi:10.2210/pdb2pzn/pdb.
- [40] H. Steuber, An old NSAID revisited: crystal structure of aldose reductase in complex with sulindac at 1.0 Å supports a novel mechanism for its anticancer and antiproliferative effects, *ChemMedChem* 6 (2011) 2155–2157.
- [41] M.C. Van Zandt, M.L. Jones, D.E. Gunn, L.S. Geraci, J.H. Jones, D.R. Sawicki, J. Sredy, J.L. Jacot, A.L. Dicioccio, T. Petrova, A. Mitschler, A.D. Podjarny, Discovery of 3-[(4,5,7-trifluorobenzothiazol-2-yl)methyl]indole-N-acetic acid (lidorestat) and congeners as highly potent and selective inhibitors of aldose reductase for treatment of chronic diabetic complications, *J. Med. Chem.* 48 (2005) 3141–3152.
- [42] F. Ruiz, I. Hazemann, A. Mitschler, A. Joachimiak, T. Schneider, M. Karplus, A. Podjarny, The crystallographic structure of the aldose reductase–IDD552 complex shows direct proton donation from tyrosine 48, *Acta Crystallogr. D: Biol. Crystallogr.* 60 (2004) 1347–1354.
- [43] G.M. Sastry, M. Adzhigirey, T. Day, R. Annabhipimoju, W. Sherman, Protein and ligand preparation: parameters, protocols, and influence on virtual screening enrichments, *J. Comput. Aided Mol. Des.* 27 (2013) 221–234.
- [44] M. Kaur, M.S. Bahia, O. Silakari, Exploring the role of water molecules for docking and receptor guided 3D-QSAR analysis of naphthyridine derivatives as spleen tyrosine kinase (Syk) inhibitors, *J. Chem. Inf. Model.* 52 (2012) 2619–2630.
- [45] Prime, Version 3.1, Schrödinger, LLC, New York, NY, 2012.
- [46] P.A. Greenidge, C. Kramer, J.C. Mozziconacci, R.M. Wolf, MM/GBSA binding energy prediction on the PDBbind data set: successes, failures, and directions for further improvement, *J. Chem. Inf. Model.* 53 (2013) 201–209.
- [47] PHASE, Version 3.4, Schrödinger, LLC, New York, NY, 2012.
- [48] S.L. Dixon, A.M. Smolydrev, E.H. Knoll, S.N. Rao, D.E. Shaw, R.A. Friesner, PHASE: a new engine for pharmacophore perception, 3D QSAR model development, and 3D database screening. 1. Methodology and preliminary results, *J. Comput. Aided Mol. Des.* 20 (2006) 647–671.
- [49] O. Silakari, S. Chand, M.S. Bahia, Structural basis of amino pyrimidine derivatives for inhibitory activity of PKC-θ: 3D-QSAR and molecular docking studies, *Mol. Inf.* 31 (2012) 659–668.
- [50] M. Kaur, A. Kumari, M.S. Bahia, O. Silakari, Designing of new multi-targeted inhibitors of spleen tyrosine kinase (Syk) and zeta-associated protein of 70 kDa (ZAP-70) using hierarchical virtual screening protocol, *J. Mol. Graph. Model.* 39 (2013) 165–175.
- [51] S. Zhang, A. Golbraikh, S. Oloff, H. Kohn, A. Tropsha, A novel automated lazy learning QSAR (ALL-QSAR) approach: method development, applications, and virtual screening of chemical databases using validated ALL-QSAR models, *J. Chem. Inf. Model.* 46 (2006) 1984–1995.
- [52] A. Golbraikh, A. Tropsha, Beware of q2!, *J. Mol. Graph. Model.* 20 (2002) 269–276.
- [53] W. Baker, Molecular rearrangement of some o-acyloxyacetophenones and the mechanism of the production of 3-acylchromones, *J. Chem. Soc.* 10 (1933) 1381–1389.
- [54] H.S. Mahal, K. Venkataraman, Synthetical experiments in the chromone group. Part XIV. The action of sodamide on 1-acyloxy-2-acetonaphthones, *J. Chem. Soc.* 10 (1934) 1767–1769.
- [55] S. Hayman, J.H. Kinoshita, Isolation and properties of lens aldose reductase, *J. Biol. Chem.* 240 (1965) 877–882.
- [56] S. Gupta, N. Singh, A.S. Jaggi, Evaluation of in vitro aldose reductase inhibitory potential of alkaloidal fractions of *Piper nigrum*, *Muraya koenigii*, *Argemone mexicana*, and *Nelumbo nucifera*, *J. Basic Clin. Physiol. Pharmacol.* 24 (2013) 1–11.

- [57] M.S. Bahia, S.K. Gunda, S.R. Gade, S. Mahmood, R. Muttineni, O. Silakari, Anthranilate derivatives as TACE inhibitors: docking based CoMFA and CoMSIA analyses, *J. Mol. Model.* 17 (2011) 9–19.
- [58] M.S. Bahia, O. Silakari, 3D-QSAR analysis of benzimidazole inhibitors of interleukin-2 inducible T cell kinase (ITK) considering receptor flexibility and water importance for molecular alignment, *Med. Chem. Res.* 22 (2013) 5578–5587.
- [59] B. Vyas, O. Silakari, M.S. Bahia, B. Singh, Glutamine: fructose-6-phosphate amidotransferase (GFAT): homology modelling and designing of new inhibitors using pharmacophore and docking based hierarchical virtual screening protocol, *SAR QSAR Environ. Res.* 24 (2013) 733–752.